TITLE
ASP Conference Series, Vol. **VOLUME***, **YEAR OF PUBLICATION**
NAMES OF EDITORS

Recent Progress on a New Distance to NGC 4258

E.M.L. Humphreys, A.L. Argon, L.J. Greenhill, J.M. Moran, M.J. Reid

Harvard-Smithsonian Center for Astrophysics, 60 Garden Street, Cambridge, MA 02138

Abstract. We report on our ongoing, high-resolution study of H_2O masers in the innermost parsec of NGC 4258. Over thirty epochs of VLBA and VLA data, taken over six years, are being used to monitor the velocities, accelerations, positions and proper motions of water masers rotating in a warped, Keplerian disk about a supermassive central object. Our extensive monitoring results in an improved accuracy in the distance determination to this galaxy (i) via a reduction in experimental random errors due to a longer time-baseline than in previous work; and (ii) via a better modeling of sources of systematic error, such as disk eccentricity. These data can therefore yield an extremely accurate geometric distance to NGC 4258.

1. Introduction

NGC 4258 is a nearby (∼7 Mpc) Seyfert 2/LINER that has been extensively studied in recent years due to a sub-parsec, circumnuclear disk revealed by VLBA water maser observations at 22 GHz (Miyoshi at al. 1995; Herrnstein et al. 1999, H99 hereafter). The current picture of the maser disk stems from the contributions of several groups. Notably, Nakai et al. (1993) discovered the existence of high-velocity features in the 22 GHz spectrum, at $v_{sys}\pm1000$ km s^{-1}, providing an indication that the maser emission could be originating from a rotating disk. Subsequent single-dish monitoring programs measured widespread velocity drifts in the systemic emission of ∼9 km s^{-1} yr^{-1}, whereas negligible drifts were seen for the high-velocity spectral outliers (Haschick et al. 1994; Greenhill et al. 1995a; Nakai et al. 1995). These data were found to be consistent with the line-of-sight centripetal accelerations expected for masers located in a disk, rotating about a supermassive black hole (∼4 10^7 $M_\odot$) at ∼7 Mpc. In this interpretation (Watson & Wallin 1994; Greenhill et al. 1995b; Moran et al. 1995), the high-velocity maser features should be very close to, or located on, the mid-line of the disk (the diameter where the sky plane intersects the disk) and the systemic masers are located on the front side. The existence of a disk of sub-pc extent was confirmed by Miyoshi et al. (1995) using the VLBA in observations which showed that the rotation curve of the high-velocity masers is very close to Keplerian (to <1 %). Multi-epoch VLBA observations led to the measurement of proper motions for the systemic features of ∼30 μas yr^{-1} (H99), data consistent with the interpretation that the maser gas is moving ballistically in the rotating disk of NGC 4258.

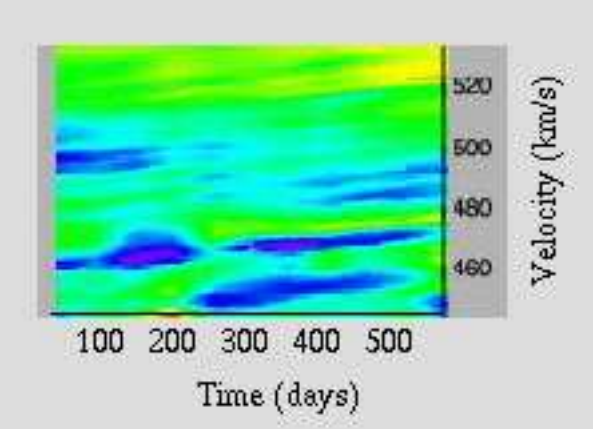

Figure 1. Flux density as a function of Doppler velocity and time for a portion of the systemic maser spectrum measured at 12 epochs between 1998-2000. The maximum flux density is around 6 Jy, represented by the darkest grayscale in this plot.

2. This Work: A New Distance

H99 measured a "geometric" distance of 7.2±0.5 Mpc to NGC 4258. The 7 % error in this quantity includes components from both random and systematic errors, with the systematic error dominating over the random component by a factor of 2. This distance was calculated from 4 epochs of VLBA data taken over 3 years. Significantly, H99 found the *same answer for the distance to within ∼1% using two broadly independent methods*, one using the maser feature accelerations and the other using the proper motion data.

With such an accurate distance to NGC 4258, an obvious question is why pursue this number to an even greater accuracy? The answer is the role that the geometric distance to this galaxy could play in the calibration of the extragalactic distance scale i.e. that NGC 4258 might replace the still controversial distance to the LMC as the anchor for the zero point in the Cepheid calibration. It has the potential to do this with great accuracy, obtaining a value for H_0 which is accurate to 5% or better, if we can drive down the total error in the geometric distance measurement by a factor of 2 - 3. To date, we have been working on reducing the random component of the error and will address the reduction of systematic errors in a later paper. We can achieve this (i) by increasing the number of epochs and (ii) by increasing the time baselines in our dataset (since $\sigma_{random} \propto N_{epochs}^{-1/2}(N_{epochs}\Delta T)^{-1}$). So far, we have increased the number of epochs to 17 imaging epochs that resolve the disk structure and 36 epochs that provide spectra (17 VLBA, 14 VLA, 5 Effelsberg) over a duration of 6 years.

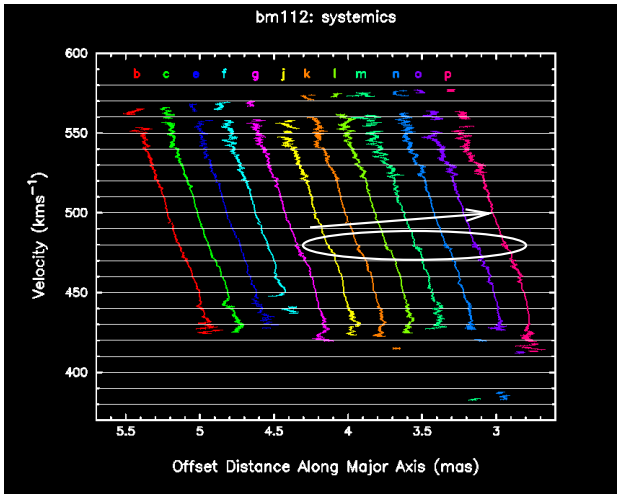

Figure 2. Rotation curve for systemic maser emission at each epoch of observation. Different epochs have been offset along the x-axis for clarity.

3. New VLBA Additions to the Dataset

In this section we highlight the most recent additions to our archive, 12 epochs of VLBA data taken over 2 years (1998-2000). Figure 1 shows a portion of the systemic maser spectra from these data. It is clear from this Figure that some systemic maser features persist throughout the two years, and also that they undergo a drift in Doppler velocity. The velocity-position diagram for systemic masers is shown in Figure 2. In Figure 2, it is evident that substructure in the disk exists, that is persists between epochs, and that it changes velocity consistent with the centripetal acceleration of the disk. We believe that this provides further evidence that we are tracking 'persistent features' moving in the disk. Figure 3 goes on to show the rotation curve for the 12 epochs plotted overlaid, the arrow pointing to the new detection of masing material at the highest velocity that has ever been observed, at 1562 km s^{-1}. This feature, whose sky position is marked by the circle in Figure 4, is now the closest high-velocity maser feature to the center of the disk. This means that the inner edge of the high velocity features quite closely corresponds to the disk radius of the systemic features, but does not lie inside this radius (cf H99).

Table 1. Current best-fit parameters for maser disk (χ^2=1.8), see text for label definitions.

v_{sys} (kms^{-1})	x_0 (mas)	y_0 (mas)	M/D ($10^7 M_\odot$ Mpc^{-1})	α_0 (deg)	α_1 (deg mas^{-1})	α_2 (deg mas^{-2})	i_0 (deg)	i_1 (deg mas^{-1})
474.1	−0.132	0.548	0.526	65.3	2.3	−0.23	71.6	2.4

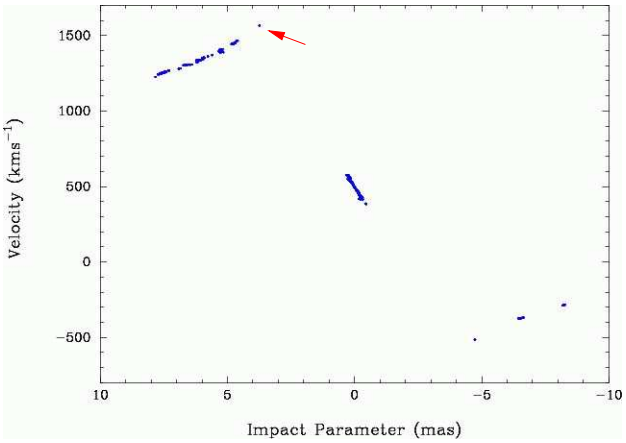

Figure 3. Rotation curve for the 12 epochs of data overlaid, including the high-velocity features. The arrow points to the newly-detected, highest velocity feature at 1562 km s^{-1}.

4. From Data to Distance

In order to calculate the distance, we require maser feature accelerations or/and proper motions and the polar coordinates of maser features in the disk. We describe how the necessary quantities are obtained below.

(i) Accelerations & Proper Motions: The method used here to measure feature accelerations and proper motions differs from that used by H99. Since the time intervals between epochs were relatively long in H99, and the number of epochs limited to 4, individual features in the spectra or images could not be tracked 'by eye'. Instead a Bayesian analysis technique was employed in order to match up maser features between epochs, resulting in measured accelerations and proper motions. Since we have a more frequent time sampling, over a longer time baseline, we are able to track unambiguously spectral features between epochs. This is achieved in practice by using a non-linear, Gaussian fitting routine which decomposes *simultaneously* the spectra of up to 36 epochs of data into individual Gaussians, each corresponding to a maser 'feature'. The routine fits for feature Doppler velocity (which can be used to determine accurate sky positions for the proper motion measurements) and amplitude. It also fits for feature line-of-sight acceleration, provided by the drift in Doppler velocities of each feature among epochs, and the time derivative of this quantity, i.e the jerk.

(ii) Maser Disk Coordinates: The deprojection of maser features from the sky plane requires the construction of a 3D disk model that introduces the disk-modeling systematic errors to the distance measurement. In order to deproject the maser sky positions we employ a 9-parameter χ^2 fitting routine which fits for the systemic, galactic velocity (v_{sys}), dynamical disk center (x_0,y_0), black hole mass/distance ($\mathcal{M}$=M/D), position angle warping ($\alpha(\theta_r) = \alpha_0 + \alpha_1\theta_r + \alpha_2\theta_r^2$; α measured East of North) and inclination angle warping ($i(\theta_r) = i_0 + i_1\theta_r$) where θ_r is the radial distance in the disk in angular units. A "genetic" algorithm is employed in order to find the global minimum for this fit, in which

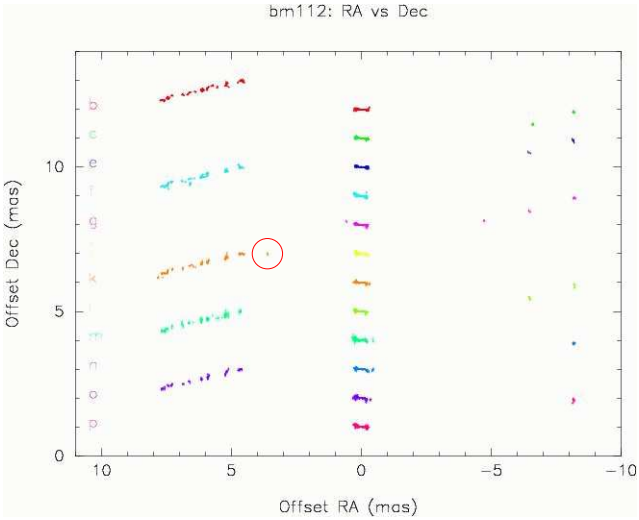

Figure 4. Sky positions for the maser emission at each epoch. Note that the redshifted features were observed for 5 of the 12 epochs; the blueshifted features were observed for 7 epochs. The circle marks the position of the highest velocity feature at 1562 km s^{-1}.

the VLBA data from all 12 epochs is included. Table 1 shows that the best fit to date indicates that *the maser disk is significantly warped* (H99 and references therein; Herrnstein et al. 2003). This process yields (θ_r,ϕ; ϕ measured from the disk midline), the angular polar disk coordinates for each maser feature, for the fit that has resulted in the smallest value of χ^2.

We now have all the quantities required to calculate the distance since, using centripetal acceleration, the distance is given by a weighted mean of $D = G\mathcal{M}\cos(\phi)\sin(i(\theta_r))/(\theta_r^2\dot{v}_{los})$ for maser features, where G is the gravitational constant. **In conclusion, a preliminary analysis indicates that so far we have succeeded in reducing the random component of the distance error to a third of its previous value. The total error (random + systematic) on the distance measurement to NGC 4258 has now been reduced from 7% to 5.5%.**

References

Greenhill, L. J., Henkel, C., Becker, R., et al., 1995a, A&A, 304, 21
Greenhill, L. J., Jiang, D. R., Moran, J. M., Reid, M. J., et al., 1995b, ApJ, 440, 619
Haschick, A. D., Baan, W. A., Peng, E. W. 1994, ApJ, 437, L35
Herrnstein, J. R., Moran, J. M., Greenhill, L. J., et al., 1999, Nat., 400, 539 (H99)
Herrnstein, J. R., Moran, J. M., Greenhill, L. J., Trotter A. S., 2003, in prep
Miyoshi, M., Moran, J. M., Herrnstein, J. et al., 1995, Nat., 373, 127
Moran, J. M., Greenhill, L. J., Herrnstein, J., et al., 1995, PNAS, 921, 1427
Nakai, N., Inoue, M., Miyoshi, M., 1993, Nat., 361, 45
Nakai, N., Inoue, M., Miyazawa, K., et al., 1995, PASJ, 47, 771
Watson, W.D., Wallin, B.K. 1994, ApJ, 432, L35